Published in final edited form as:
Cleft Palate Craniofac J. 2008 November ; 45(6): 571–582. doi:10.1597/07-095.1.

Comparison of Craniofacial Phenotype in Craniosynostotic Rabbits Treated With Anti–Tgf-β2 at Suturectomy Site

Brenda C. Frazier, M.A. [graduate student],
Department of Anthropology, Pennsylvania State University, University Park, Pennsylvania

Mark P. Mooney, Ph.D. [Professor],
Departments of Oral Biology, Anthropology, Plastic and Reconstructive Surgery, and Orthodontics, and is affiliated with the Cleft Palate-Craniofacial Center, University of Pittsburgh, Pittsburgh, Pennsylvania

H. Wolfgang Losken, F.R.C.S. (Edin.) [Clinical Professor],
Department of Plastic Surgery, School of Medicine, University of North Carolina, Chapel Hill, North Carolina

Tim Barbano [Research Specialist],
Department of Anthropology, University of Pittsburgh, Pittsburgh, Pennsylvania

Amr Moursi, D.D.S., Ph.D. [Associate Professor and Chair],
Department of Pediatric Dentistry, College of Dentistry, New York University, New York, New York

Michael I. Siegel, Ph.D. [Professor], and
Departments of Anthropology and Orthodontics, University of Pittsburgh, Pittsburgh, Pennsylvania

Joan T. Richtsmeier, Ph.D. [Professor]
Department of Anthropology, Pennsylvania State University, University Park, Pennsylvania

Abstract

Objective—Overexpression of transforming growth factor-beta 2 has been associated with craniosynostosis and resynostosis following surgery. We examined the effects of localized transforming growth factor-beta 2 inhibition on craniofacial phenotype in rabbits with craniosynostosis.

Design—Twenty-five New Zealand white rabbits with bilateral coronal craniosynostosis were divided into three treatment groups: (1) suturectomy control (n = 8); (2) suturectomy with nonspecific, control immunoglobulin G antibody (n = 6); and (3) suturectomy with anti–transforming growth factor-beta 2 antibody (n = 11). At 10 days of age, a coronal suturectomy was performed on all rabbits. The sites in groups 2 and 3 were immediately filled with a slow-resorbing collagen gel mixed with either immunoglobulin G or anti–transforming growth factor-beta 2 antibody. Computed tomography scans of each rabbit were acquired at ages 10, 25, and 84 days. Craniofacial landmarks were collected from three-dimensional computed tomography reconstructions, and growth and form were compared among the three groups.

Results—Rabbits treated with anti–transforming growth factor-beta 2 antibody differed in form at 84 days of age compared with suturectomy control rabbits, specifically in the snout and posterior neurocranium. Growth in some areas of the skull was greater in rabbits from the anti–transforming

Address correspondence to: Brenda Frazier, Department of Anthropology, 409 Carpenter Building, Pennsylvania State University, University Park, PA 16802. bcf134@psu.edu.

Presented in part at the 61st annual meeting of the American Cleft Palate-Craniofacial Association, March 2004, Chicago, Illinois.

growth factor-beta 2 group than in suturectomy control rabbits, but not significantly greater than in IgG control rabbits.

Conclusions—We find support for the hypothesis that transforming growth factor-beta 2 inhibition alters adult form, but these changes do not appear to be localized to the suturectomy region. Slight differences in form and growth between the two control groups suggest that the presence of the collagen vehicle itself may affect skull growth.

Keywords

coronal suturectomy; craniosynostosis; craniofacial; rabbits; Tgf-β2

Craniosynostosis (i.e., premature fusion of one or more cranial sutures) impedes normal growth and development of the neurocranium and may result in associated abnormalities of the craniofacial complex (Babler, 1989; Cohen, 2000c; Richtsmeier, 2002). In humans, 95% of brain growth is completed by 6 years of age (Enlow, 1990), by which time the metopic suture has fused in about 90% of individuals. The remaining cranial sutures will not fuse fully until well into adulthood (Cohen, 2000b). The full impact of craniosynostosis on neurological development is not well understood. The early closure of even a single suture is widely thought to increase intracranial pressure (ICP) (Renier, 1989; Gault et al., 1992; Campbell et al., 1995; Thompson et al., 1995; Pollack et al., 1996; Hudgins et al., 1998; Mooney et al., 1998a, 1999; Jane and Persing, 2000; Fellows-Mayle et al., 2004), although this finding has been questioned because normative ICP data are rare (Cohen and Persing, 1998; Mouradian, 1998) and accurately assessing continuous ICP recordings is problematic (Eide et al., 2002). Simple, nonsyndromic craniosynostosis occurs at a frequency estimated at 300 to 500 per 1,000,000 live births, of which approximately one fifth are instances of coronal suture synostosis (Cohen, 2000a). Calvarial growth generally is impeded in the direction perpendicular to the affected suture and is enhanced in the parallel direction (Virchow, 1851; Jane and Persing, 2000). In bilateral coronal suture synostosis, these altered growth patterns produce a characteristically brachycephalic shape of the head: anteroposteriorly shortened, mediolaterally widened, and superoinferiorly expanded (Jane and Persing, 2000). Extreme brachycephaly resulting from coronal suture synostosis is observed both in humans (Delashaw et al., 1989) and in rabbits (Mooney et al., 1994b; Burrows et al., 1999).

Congenital coronal suture synostosis is well studied in the New Zealand white rabbit (*Oryctolagus cuniculus*) (e.g., Mooney et al., 1994a, 1994b, 2001; Burrows et al., 1999). The coronal suture starts to fuse by 21 days of gestation (Mooney et al., 1996), and the anterior fontanelle and coronal suture are obliterated by 10 days of age in rabbits affected by early-onset coronal suture fusion (Mooney et al., 1994b). A slightly elevated bony ridge along the suture and frontal “bossing” also are observed, with shortening and widening of the cranial vault. In extreme cases, Mooney et al. (1994b) have reported the occurrence of “midfacial hypoplasia resulting in malocclusion and incisal overgrowths” (p. 3). A morphometric study by Burrows et al. (1999) found that in adult rabbits with unoperated, complete coronal synostosis, the cranial vault was significantly shorter than in unaffected individuals, and the parietal and frontal bones were shorter and wider.

Current treatment protocols for craniosynostosis in humans typically include some formof neurocranial surgery. Surgical therapy in coronal craniosynostosis routinely involves complete remodeling of the skull, due to the ineffectiveness of strip craniectomy in producing a normal head shape, although other surgical techniques have grown in popularity in recent years (Jane and Persing, 2000; Yano et al., 2006; Clayman et al., 2007). Even after total reconstruction of the skull, the area representing the suture may re-fuse shortly after surgery, requiring further surgical correction in some cases (Mommaerts et al., 2001; Panchal and Uttchin, 2003). Given the invasiveness of such procedures and the morbidity associated with craniofacial surgery, it

would be advantageous to be able to prevent resynostosis and to reduce the likelihood of additional surgical procedures. Advances in understanding the etiology of craniosynostosis offer hope for more effective treatments.

Studies by Roth et al. (1997a, 1997b), Opperman et al. (1997, 2000), and others (Lin et al., 1997; Poisson et al., 2004; Lee et al., 2006) indicate that overexpression of transforming growth factor-beta 2 (Tgf-β2)[1] may be associated with premature suture fusion in humans and in animal models. Tgf-β2 is one in a family of growth regulatory molecules secreted by the dura mater that control osteogenic processes in cranial sutures (Cohen, 2000d; Warren and Longaker, 2001; Opperman and Ogle, 2002; Cohen, 2003). Although the pathogenesis of simple, nonsyndromic craniosynostosis is not well understood, Loeys et al. (2005) show that mutations in TGF-β receptor 1 and 2 are associated with some cases of craniosynostosis in humans, and experimental manipulations of Tgf-β isoforms in various studies (Mehrara et al., 2002; Chong et al., 2003) corroborate their importance in maintenance of cranial suture patency and fusion. Specifically, inhibition of Tgf-β2 using neutralizing antibodies in rat calvariae has successfully rescued normally fusing sutures from obliteration *in vitro* (Opperman et al., 1999; Moursi et al., 2003).

Building upon this previous work, we explored how treatment to inhibit Tgf-β2 at the suturectomy site affects growth of the neurocranium in a rabbit model *in vivo*. Using the same rabbit colony, Mooney et al. (2007a) demonstrated that anti–Tgf-β2 treatment delays postoperative resynostosis of the coronal suture. They also showed that, as expected, more cranial growth occurs in the anteroposterior (A–P) direction, and intracranial volume is significantly higher by 84 days of age than without antibody treatment (Mooney et al., 2007b). The present study is the first quantitative, three-dimensional comparison of overall craniofacial phenotype in these antibody treatment groups. The results of intracranial volume comparisons, two-dimensional measurements of lateral radiographs, and histology of suture tissue strongly suggest that significant differences in craniofacial growth occur in treated rabbits. We expected to find differences in form and growth associated with prolonged suture patency, particularly in the cranial vault (i.e., in the vicinity of the coronal suture).

Specifically, we hypothesized that anti–Tgf-β2–treated rabbits would exhibit less compensatory mediolateral and dorsoventral growth of the cranial vault than occurred in the control subjects. Additionally, the increased A–P growth of the skull demonstrated previously in treated rabbits (Mooney et al., 2007b) should be localized to the neurocranium. To test these hypotheses experimentally, we used three-dimensional landmark coordinate data obtained from computed tomography (CT) scans to compare the phenotype of three groups of craniosynostotic rabbits at two points following treatment.

MATERIALS AND METHODS

Sample

Twenty-five New Zealand white rabbits (*O. cuniculus*) with familial, early onset, bilateral coronal suture synostosis were considered in this study. All rabbits were born in the ongoing breeding colony of congenitally synostosed rabbits at the University of Pittsburgh in the Department of Anthropology vivarium. The synostosed rabbits from this colony share important morphological features with human infants exhibiting congenital bicoronal craniosynostosis. Phenotypically, these rabbits show bony bridging at the coronal sutures as early as 21 days gestation, obliterated coronal sutures at birth, coronal ridging, and

[1]We have adopted the convention used by Moursi et al. (2003) in abbreviating both the gene product and antibody against it with only the first letter capitalized: Tgf-β2.

brachycephalic cranial vaults by 10 days of age, and secondary changes in the cranial base, brain, and intracranial volume by 42 days of age (Mooney et al., 1994a, 1994b, 1998b, 2002).

Because this species displays very minimal sexual dimorphism (Fox, 1994), individuals were selected and studied without regard to sex. Rabbits were assigned randomly to one of three treatment groups: (1) suturectomy with no treatment, which served as the surgical control group (n = 8); (2) suturectomy with nonspecific, control immunoglobulin G (IgG) antibody in a slow-release collagen vehicle, which served as the antibody control group (n = 6); and (3) suturectomy with anti–Tgf-β2 antibody in a slow-release collagen vehicle, which served as the treatment group (n = 11). This study was reviewed and approved by the University of Pittsburgh Institutional Animal Care and Use Committee.

Surgery

At approximately 10 days of age (range = 8 to 13 days), all rabbits were anesthetized with an intramuscular (IM) injection (0.59 mL/kg) of a solution of 91% Ketaset (ketamine hydrochloride, 100 mg/mL; Aveco Co., Inc., Fort Dodge, IA) and 9% Rompun (xylazine, 20 mg/mL; Mobay Corp., Shawnee, KS). The scalps were then shaved, depilated, and prepared for surgery. The calvariae were exposed using a midline scalp incision, and the skin reflected laterally to the supraorbital borders. All animals received postoperative IM injections (2.5 mg/kg) of Baytril (Bayer Corp., Shawnee Mission, KS) as a prophylaxis for infection. A 3-mm–long by 15-mm–wide strip of frontal and parietal bones, including the entire length and width of the synostosed coronal suture, was extirpated and removed in one piece from pterion to pterion using a cutting burr. Care was taken to preserve the meningeal (fibrous) layer of the dura and the regional vascularity.

Rabbits in the suturectomy control group received a suturectomy only. The periosteal and skin incisions were then closed with 4-0 resorbable Vicryl suture (Ethicon, Somerville, NJ). For rabbits in the other two groups, the suturectomy sites were filled immediately with 0.1 mL of a slow resorbing collagen gel mixed with either IgG antibody (100 μg/suture) or anti–Tgf-β2 antibody (100 μg/suture). The collagen vehicle was a highly purified, slow-resorbing (>63 days in rabbit perisutural tissues [Moursi et al., 2003; Mooney et al., 2004]), bovine collagen type I gel and was provided by NeuColl, Inc. (Campbell, CA). The gel is approved by the U.S. Food and Drug Administration for human subdermal application and was supplied at a density of 65 mg/mL, which is much higher than other collagen gels (Moursi et al., 2003; Mooney et al., 2004). The IgG antibody is available commercially from R & D Systems (affinity purified polyclonal antibody, catalog no. G-101-CABS; Minneapolis, MN). The anti–Tgf-β2 antibody also was obtained from R & D Systems (affinity purified polyclonal antibody, catalog no. AF-302-NA; neutralization data and other details available from the manufacturer at www.rndsystems.com). The antibodies were mixed, under sterile conditions, with 100 μL aliquots of the collagen gel to a final concentration of 100 μg per gel aliquot in a 1-mL syringe. This volume ensured that the entire suturectomy site was filled with vehicle and antibody. Following injections, the periosteal and skin incisions were closed with 4-0 resorbable Vicryl suture (Ethicon).

Data Collection

Within 2 days following surgery (range = 9 to 14 days old), CT scans were acquired of each rabbit in the sagittal plane using a GE HiSpeed Advantage Scanner (display field of view = 24.0 to 18.0 cm; mA = 120 to 150; kV = 120) at a thickness of 1 mm (10-day scan). Three-dimensional CT scans were taken with the rabbits tranquilized with an IM injection (0.40 mL/kg) of a solution of 91% Ketaset (ketamine hydrochloride, 100 mg/ml; Aveco) and 9% Rompun (xylazine, 20 mg/mL; Mobay). Approximately 2 weeks later (range = 21 to 27 days old), rabbits were rescanned (25-day scan). Finally, scans were obtained at approximately 84 days of age

(84-day scan), by which time 80% to 90% of calvarial and brain growth is completed in the rabbit (Harel et al., 1972; Mooney et al., 1994a, 2001, 2002).

The visualization and analysis software eTDIPS (http://clinicalcenter.nih.gov/cip/software/etdips/) was used to produce three-dimensional reconstructions of rabbit skulls from CT slice images (Fig. 1). Nineteen bony landmarks (Fig. 2; Table 1) were identified and their coordinate locations were recorded from each skull using the eTDIPS landmarking tool. (For a more detailed description of the use of eTDIPS in collecting landmark data, see Williams and Richtsmeier [2003].) Six midline and seven paired ectocranial landmarks were chosen, based on visibility in all age groups, accuracy, and relevance to overall cranial morphology. The resolution of the medical CT scanner relative to the small size and minimal ossification of juvenile rabbits limited potential landmark choices, as well as the precision of determining landmark locations, across all age groups. For instance, no cranial sutures were consistently visible, eliminating the possibility for landmarks to be taken at discrete tissue intersections (e.g., bregma).

All data were collected by a single observer (B.C.F.). Before beginning primary data collection, an error study was conducted to assess measurement error in the landmark coordinate data. Landmark locations were recorded three separate times on each of 12 CT scan reconstructions of 10-, 25-, and 84-day-old rabbits. The mean x-, y-, and z-coordinates from the three collection trials were calculated for each landmark, and the standard deviation from the mean was computed for each axis. Landmarks with standard deviations of 0.8 mm or more in the x-, y-, or z-planes were discarded, leaving 19 landmarks for primary data collection. Following primary data collection of these landmarks in two trials, data were checked and individual landmarks were re-collected as needed to ensure that landmark data from the two trials differed by less than 0.5 mm on all three axes. The average of the x-, y-, and z-coordinates from the two digitizations was used for analysis.

Methods of Analysis

Three-dimensional coordinate landmark data were analyzed using Euclidian distance matrix analysis (EDMA; available for download at http://getahead.psu.edu/) (Lele and Richtsmeier, 1995, 2001). Form was compared within age groups and growth trajectories were compared between treatment groups (Table 2).

Test of Form Difference

The form of an object can be defined as “the characteristic that remains invariant under any translation, rotation or reflection of the object” (Lele and Richtsmeier, 2001, p. 73). This includes the concepts of both size and shape. To compare form between any two groups, EDMA converts matrices of the three-dimensional landmark coordinate data into matrices of all possible unique interlandmark distances. From these, a matrix of mean interlandmark distances is computed for each sample (an average form matrix [FM]). Then the mean value of each linear distance in a sample is compared with the corresponding mean value for the same linear distance in the other sample as a ratio. The ratio values are contained in a form difference matrix (FDM). A nonparametric boot-strapping algorithm estimates confidence intervals (CIs) for each interlandmark distance in order to evaluate the null hypothesis of similarity, distance by distance. In these analyses of form and growth, a 90% CI was constructed ($\alpha = .10$, rather than the more commonly used $\alpha = .05$) because the samples are small. Although the narrower CI increases the probability of type I error (i.e., falsely rejecting the null hypothesis of similarity), it is a more stable estimate of the true parameter when very small sample sizes are involved (Lele and Richtsmeier, 1995).

Comparison of Growth Patterns

Richtsmeier and Lele (1993) defined *growth pattern* as "the composite of geometric changes in structure occurring through time" (p. 382). Here, we evaluated growth patterns by quantifying the relative change in linear distances across time. Growth patterns were statistically compared by determining if the relative change in linear distances across time was significantly greater (or smaller) in one treatment group relative to the other group using a nonparametric bootstrapping procedure. EDMA does this by computing a growth matrix (GM) that compares the FMs of a treatment group at both an earlier and a later age as a ratio (the same calculation as the FDM in form tests). To compare relative growth against another treatment group, GMs for both groups are used to create a growth difference matrix (GDM). The GDM calculates a ratio of the two GMs, that is, the relative change recorded for each linear distance over the time interval. For example, the change in each interlandmark distance between 10 days and 84 days in the anti–Tgf-β2 group would be the numerator of a ratio comparing that group's growth to the change in each distance in the suturectomy control group over the same interval (in the denominator). If the relative growth of a given distance in the anti–Tgf-β2 group is greater over the specified time period, the ratio will be greater than 1 for that distance. If the suturectomy control group grows more in an interlandmark distance, that ratio will be less than 1. Collectively, these localized growth ratios enable comparison of relative growth patterns (Richtsmeier and Lele, 1993).

RESULTS

The CT scan data were acquired as part of a larger longitudinal study, and we chose those scans that fit our requirements for age of the individual and scan quality. Missed or unreadable scans, the timing of scans, and the early death of some rabbits meant that more than half the sample comprised individuals (14 of 25 rabbits) for which all three scans were not available. Thus, sample size varied for each age group depending on the scans available within each age range (Table 3). This also resulted in comparisons of a mixture of cross-sectional and longitudinal data. For the purposes of analysis, data were considered to be cross-sectional. This is the default assumption on which EDMA tests are based.

Statistical Significance

In this study, a linear distance must meet three significance criteria to be reported: (1) the mean estimate differs by at least 3.0% between the two samples being compared, (2) the 90% CI (of the form or growth difference ratio) for that distance excludes the value 1.0 (lower bound $\geq$1.010 or upper bound $\leq$0.990), and (3) the distance must have an average magnitude of more than 10 mm in the smallest rabbit sample used in the comparison. These criteria attempt to mitigate as much as possible the effects of landmark error, small sample size, and intragroup variability.

Intergroup Form Comparisons

At the time of the 25-day scan, approximately 2 weeks after treatment, there were no statistically significant differences in form between the suturectomy control rabbits and either of the other two groups. The only significant differences in form between members of the anti–Tgf-β2 treatment and IgG control groups were very small in magnitude (<5.0%; see Table 4; Fig. 3).

By the 84-day scan, statistically significant form differences were detectable among the three groups. Anti–Tgf-β2 rabbits differed significantly from the suturectomy control group in many distance measures. Anti–Tgf-β2 rabbits had a longer anterior portion of the cranium—especially in the snout and palate—and a wider posterior neurocranium (black and dotted lines in Fig. 4). Between antibody-treated and suturectomy control rabbits, 14 distances were

significantly different by 3.4% to 4.0%, and 27 by greater than 4.0% (see Table 5). Several statistically significant differences in form were found between the anti–Tgf-β2 and the IgG control groups in the anterior basicranium and posterior neurocranium, ranging from 3.0% to 4.8% in magnitude (see Table 6; white lines in Fig. 4). Finally, 84-day suturectomy controls were significantly larger (by 4.5% to 5.0%) than IgG controls in two dimensions of the posterior neurocranium (black lines in Fig. 5; summary statistics in Table 7).

Growth Comparisons

Form and growth were analyzed in this study, working under the hypothesis of similarity among the three treatment groups at the time of surgery and treatment (10 days of age), although the especially small number of useable 10-day scans precluded a statistically meaningful verification of this assumption (particularly for the IgG control group; n = 2). As such, all 10-day scans were pooled into a single group for growth analyses.

Growth over the first interval, from 10 to 25 days of age, did not differ significantly among the three groups in any dimension, although the form difference ratio value was above 1.0 for nearly all distances in comparisons of anti– Tgf-β2 rabbits with both control groups. Between 25 and 84 days, the only statistically significant difference in growth was in one distance of the neurocranium (between landmarks 16 and 18), where the suturectomy control group grew an average of 6.3% more than the IgG group did (a difference of about 1.25 mm; line marked with an asterisk in Fig. 5).

Over the full duration of the study (10 to 84 days), statistically significant differences in growth occur between anti–Tgf-β2 rabbits and the suturectomy control group. Anti–Tgf-β2 rabbits grew significantly more than suturectomy controls in width dimensions of the posterior cranium, as well as in length of the upper face (Table 8; Fig. 6). As in the 25- to 84-day interval, suturectomy control individuals grew significantly more (by an average of 5.0%) than IgG controls in a single neurocranial dimension (marked with an asterisk in Fig. 5). A single significant difference in growth is detected in this same dimension (see asterisk in Fig. 5) between anti–Tgf-β2 and IgG control individuals over the study period. The rabbits receiving anti–Tgf-β2 treatment grew an average of 4.8% more than IgG controls in this distance, a difference of about 1.11 mm.

DISCUSSION

The results are broadly consistent with the expectation that treatment with Tgf-β2 neutralizing antibodies following surgical release of a prematurely fused coronal suture will result in different three-dimensional adult form than will surgery alone in a rabbit model. The crania of juvenile rabbits treated with anti–Tgf-β2 antibodies in a slow-release collagen vehicle are slightly larger in several dimensions compared with both control groups by 84 days of age. This is consistent with Mooney and colleagues' (2007a, 2007b) findings of prolonged patency at the coronal suture and increased intracranial volumes in rabbits treated with anti–Tgf-β2. One caveat to this is that growth differences between anti–Tgf-β2 rabbits and those given the nonspecific (IgG) antibody were not statistically significant, except in one distance used in these analyses. This raises the issue of biological as opposed to statistical significance. We have clear evidence that adult form is different in anti–Tgf-β2 rabbits than in rabbits in either control group (corroborated by Mooney and colleagues' [2007b] findings), so differential growth must be occurring. The magnitude of these changes, however, must be too small to be detectable as statistically significantly different in these samples. Thus, we can be fairly confident that inhibition of Tgf-β2 does affect growth beyond what may be attributed to the effects of the collagen alone, but the practical constraints of this study (including sample size and scan resolution) do not permit a conclusive demonstration of these effects. Further

experimental research into antibody treatment and delivery vehicles is needed to better characterize the quantitative and qualitative effects on sutures and overall craniofacial growth.

The form differences detected in adults of the antibody treatment group are probably a result of prolonged patency of the suturectomy site maintained through interference with Tgf-β2 binding activity and function. Although Tgf-β2 binding activity and function were not measured in these rabbits, these data are consistent with *in vitro* studies that show inhibition of normal rodent suture fusion by interfering with Tgf-β2 function (Opperman et al., 1999; Warren and Longaker, 2001; Opperman and Ogle, 2002; Moursi et al., 2003; Mooney et al., 2004).

Where we were able to detect increased growth in anti– Tgf-β2 compared with suturectomy controls, the differences are not especially localized to the neurocranium, according to these analyses. A few dimensions of increased growth in anti–Tgf-β2 individuals (see Fig. 6) may indirectly indicate relative neurocranial lengthening compared with suturectomy controls. There is also evidence that some of the increased growth is localized to basicranial width (Fig. 6). Contrary to our expectations, these analyses do not suggest compensatory mediolateral or dorsoventral growth of the cranial vault (i.e., along the sagittal suture) in rabbits receiving no antibody treatment compared with treated individuals. On the contrary, some differences in growth suggest that the anti–Tgf-β2 group grew more in mediolateral and dorsoventral dimensions than suturectomy controls did (Table 8; Fig. 6).

Rabbits treated with anti–Tgf-β2 exhibited longer snouts than the control groups did at 84 days, which was not expected in a region distant from the suturectomy site itself. A plausible explanation for this is that subtle differences detected in the cranial base may affect the way the palate and, hence, the snout grows in the A–P direction. It is possible that in the most severe cases of synostosis (suturectomy control rabbits), anterior extension of the snout is inhibited by abnormal growth of the cranial base. It has been shown that completely untreated (synostosed) rabbits are brachycephalic and can have malocclusion, compared with unaffected individuals (Mooney et al., 1994b; Burrows et al., 1999). Antibody therapy may ameliorate this slightly, allowing more A–P growth of the snout in the anti–Tgf-β2 group (see especially Fig. 4; Table 5 and Table 6).

We also expected that the two control groups would be indistinguishable from one another in form and in growth. Two lines of evidence contradict this expectation. First, IgG control rabbits did not differ from anti–Tgf-β2 rabbits in form or growth in the same way as suturectomy control individuals. In fact, they did not differ significantly from rabbits treated with anti–Tgf-β2 in any dimension by 5% or more. Second, in direct comparisons of form and growth, suturectomy control individuals appeared to be significantly larger in the posterior neurocranium (between landmarks 16 and 18) than rabbits receiving IgG treatment (line with asterisk, Fig. 5). The data do not provide an explanation for this apparent discrepancy.

Although we cannot construe the lack of evidence for differences with evidence for similarity, the scarcity of differences in form or growth of the IgG group compared with either of the other groups does suggest that the IgG individuals may exhibit a sort of “intermediate” form. Mature (84-day) anti–Tgf-β2 rabbits are statistically significantly larger than the suturectomy control rabbits in several distances, but only by a small magnitude (up to 6.2%, Table 5). If the IgG control rabbits are only slightly smaller than the anti–Tgf-β2 group and slightly larger than the suturectomy control group in these distances, then the IgG form could be a kind of intermediate form that is not statistically significantly different from either of the other two. There is some evidence that this is the case. Suturectomy control rabbits were somewhat smaller than IgG control individuals for most distances of the snout and face (by 3% to 4%), despite being slightly longer in a distance of the neurocranium, whereas anti–Tgf-β2 rabbits were somewhat larger

than IgG control rabbits in most distances (up to 4.8%). Mooney et al. (2007a) reported similar findings in that IgG control rabbits exhibited slightly slower reossification rates than did suturectomy control rabbits at 25 and 42 days of age, although the differences were not statistically significant. The authors suggested that this was probably not an effect of the IgG but rather was due to the presence of the collagen vehicle itself in the suturectomy site, which may have had an osteoinhibitory effect on reossification of the suturectomy site during degradation (Mooney et al., 2007a). A recent *in vitro* study (Premaraj et al., 2006) also has shown that the collagen vehicle alone had a short-term inhibitory effect on osteoblast cell number in culture. Because the ultimate goal of this research is to inhibit postoperative resynostosis and to improve craniofacial growth, this should not be viewed as a confounding variable, although future studies designed to facilitate osteogenesis using various growth factors delivered by this collagen vehicle should take this into consideration (Mooney et al., 2004,2007a,2007b;Premaraj et al., 2006). Ideally, the effects of collagen alone should be compared experimentally with treatment with collagen plus Tgf-β2 inhibition to delineate more clearly the contribution of each material to bone growth.

In considering the findings of this study, it should be noted that resynostosis was still seen in the anti–Tgf-β2 antibody treatment group before the end of the rabbit neurocranial growth phase (~84 days of age) (Mooney et al., 2007a, 2007b). This could indicate that antibody therapy delivered via a resorbable collagen vehicle may have only a transitory effect and alternative methods will have to be explored for prolonged delivery of such biological therapies (Warren et al., 2003; Mooney et al., 2004).

The results of this study and others suggest a promising role for biologically based treatments of craniosynostosis, yet obstacles remain to the use of these therapies in humans (Mooney et al., 2004, 2007a, 2007b). Foremost among these obstacles is the duration of delivery of bioreactive agents necessary for clinical utility. Humans achieve approximately 90% of their total brain growth by 2 years of age (Enlow, 1990), compared with rabbits requiring just a few weeks. In humans, therapeutic agents would have to be delivered in multiple doses using existing technologies (Boyan et al., 1999; Alsberg et al., 2001, 2002; Franceschi, 2005; Premaraj et al., 2005) or via a novel, slow-release vehicle that would last long enough to have a therapeutic effect on neurocranial growth.

CONCLUSION

These results support our initial hypothesis that antibody treatment would change craniofacial growth in this rabbit model. However, the study does not conclusively isolate significant growth effects of treatment to Tgf-β2 inhibition. We did not find evidence for a reduction in the relative magnitude of mediolateral and dorsoventral growth of the neurocranium in rabbits treated with anti–Tgf-β2 compared with those receiving suturectomy only. We also found little evidence that growth increases in anti–Tgf-β2 rabbits are localized to the suturectomy region. Nonetheless, our findings corroborate previous studies in suggesting that biologically based therapy may be a potential adjunct to the surgical treatment of infants with craniosynostosis (Kwan et al., 2007), particularly once the technological aspects of delivery systems and gene therapy are improved.

Acknowledgments

The authors would like to thank Kristina Aldridge, Cheryl Hill, and Katherine Willmore for their assistance with data analysis, interpretation, and presentation.

This work was supported in part by National Institutes of Health grants P60 DE13078, R01 DE016886, and R01 DE018500, and by a National Science Foundation Graduate Research Fellowship (B.C.F.). The collagen vehicle was provided by NeuColl Inc., Campbell, California.

REFERENCES

Alsberg E, Anderson KW, Albeiruti A, Rowley JA, Mooney DJ. Engineering growing tissues. Proc Natl Acad Sci U S A 2002;99:12025–12030. [PubMed: 12218178]

Alsberg E, Hill EE, Mooney DJ. Craniofacial tissue engineering. Crit Rev Oral Biol Med 2001;12:64–75. [PubMed: 11349963]

Babler, W. Relationship of altered cranial suture growth to cranial base and midface. In: Persing, JA.; Edgerton, MT.; Jane, JA., editors. Scientific Foundations and Surgical Treatment of Craniosynostosis. Baltimore: Williams & Wilkins; 1989. p. 87-95.

Boyan BD, Lohmann CH, Romero J, Schwartz Z. Bone and cartilage tissue engineering. Clin Plast Surg 1999;26:629–645. ix. [PubMed: 10553218]

Burrows AM, Richtsmeier JT, Mooney MP, Smith TD, Losken HW, Siegel MI. Three-dimensional analysis of craniofacial form in a familial rabbit model of nonsyndromic coronal suture synostosis using Euclidean distance matrix analysis. Cleft Palate Craniofac J 1999;36:196–206. [PubMed: 10342607]

Campbell JW, Albright AL, Losken HW, Biglan AW. Intracranial hypertension after cranial vault decompression for craniosynostosis. Pediatr Neurosurg 1995;22:270–273. [PubMed: 7547460]

Chong SL, Mitchell R, Moursi AM, Winnard P, Losken HW, Bradley J, Ozerdem OR, Azari K, Acarturk O, Opperman LA, et al. Rescue of coronal suture fusion using transforming growth factor-beta 3 in rabbits with delayed-onset craniosynostosis. Anat Rec 2003;274A:962–971.

Clayman MA, Murad GJ, Steele MH, Seagle MB, Pincus DW. History of craniosynostosis surgery and the evolution of minimally invasive endoscopic techniques: the University of Florida experience. Ann Plast Surg 2007;58:285–287. [PubMed: 17471133]

Cohen, MM, Jr. Epidemiology of craniosynostosis. In: Cohen, MM., Jr; MacLean, RE., editors. Craniosynostosis: Diagnosis, Evaluation, and Management. 2nd ed.. New York: Oxford University Press; 2000a. p. 112-118.

Cohen, MM, Jr. Sutural biology. In: Cohen, MM., Jr; MacLean, RE., editors. Craniosynostosis: Diagnosis, Evaluation, and Management. 2nd ed.. New York: Oxford University Press; 2000b. p. 11-23.

Cohen, MM, Jr. Sutural pathology. In: Cohen, MM., Jr; MacLean, RE., editors. Craniosynostosis: Diagnosis, Evaluation, and Management. 2nd ed.. New York: Oxford University Press; 2000c. p. 51-68.

Cohen MM, Jr. TGFβ and sutural biology. In: Cohen, MM., Jr; MacLean, RE., editors. Craniosynostosis: Diagnosis, Evaluation, and Management. 2nd ed.. New York: Oxford University Press; 2000d. p. 69-76.

Cohen MM Jr. TGF beta/Smad signaling system and its pathologic correlates. Am J Med Genet A 2003;116:1–10. [PubMed: 12476444]

Cohen SR, Persing JA. Intracranial pressure in single-suture craniosynostosis. Cleft Palate Craniofac J 1998;35:194–196. [PubMed: 9603551]

Delashaw JB, Persing JA, Broaddus WC, Jane JA. Cranial vault growth in craniosynostosis. J Neurosurg 1989;70:159–165. [PubMed: 2913214]

Eide PK, Helseth E, Due-Tonnessen B, Lundar T. Assessment of continuous intracranial pressure recordings in childhood craniosynostosis. Pediatr Neurosurg 2002;37:310–320. [PubMed: 12422046]

Enlow, DH. Facial Growth. Philadelphia: WB Saunders; 1990.

Fellows-Mayle WK, Mitchell R, Losken HW, Bradley J, Siegel MI, Mooney MP. Intracranial pressure changes in craniosynostotic rabbits. Plast Reconstr Surg 2004;113:557–565. [PubMed: 14758218]

Fox, RR. Taxonomy and genetics. In: Manning, PJ.; Ringler, DH.; Newcomer, CE., editors. The Biology of the Laboratory Rabbit. San Diego: Academic Press; 1994. p. 1-27.

Franceschi RT. Biological approaches to bone regeneration by gene therapy. J Dent Res 2005;84:1093–1103. [PubMed: 16304438]

Gault DT, Renier D, Marchac D, et al. Intracranial pressure and intracranial volume in children with craniosynostosis. Plast Reconstr Surg 1992;90:377–381. [PubMed: 1513883]

Harel S, Watanabe K, Linke I, Schain RJ. Growth and development of the rabbit brain. Biol Neonate 1972;21:381–399. [PubMed: 4657752]

Hudgins RJ, Cohen SR, Burstein FD, Boydston WR. Multiple suture synostosis and increased intracranial pressure following repair of single suture, nonsyndromal craniosynostosis. Cleft Palate Craniofac J 1998;35:167–172. [PubMed: 9527314]

Jane, JA.; Persing, JA. Neurosurgical treatment of craniosynostosis. In: Cohen, MM., Jr; MacLean, RE., editors. Craniosynostosis: Diagnosis, Evaluation, and Management. 2nd ed.. New York: Oxford University Press; 2000. p. 209-227.

Kwan MD, Wan DC, Longaker MT. Discussion of "Anti-TGF-beta2 antibody therapy inhibits postoperative resynostosis in craniosynostotic rabbits.". Plast Reconstr Surg 2007;119:1213–1215.

Lee SW, Choi KY, Cho JY, Jung SH, Song KB, Park EK, Choi JY, Shin HI, Kim SY, Woo KM, et al. TGF-beta2 stimulates cranial suture closure through activation of the Erk-MAPK pathway. J Cell Biochem 2006;98:981–991. [PubMed: 16795080]

Lele S, Richtsmeier JT. Euclidean distance matrix analysis: confidence intervals for form and growth comparison. Am J Phys Anthropol 1995;98:73–86. [PubMed: 8579192]

Lele, SR.; Richtsmeier, JT. An Invariant Approach to Statistical Analysis of Shapes. Boca Raton, FL: Chapman & Hall/CRC; 2001.

Lin KY, Nolen AA, Gampper TJ, Jane JA, Opperman LA, Ogle RC. Elevated level of transforming growth factor β2 and β3 in lambdoid sutures from children with persistent plagiocephaly. Cleft Palate Craniofac J 1997;34:331–337. [PubMed: 9257024]

Loeys BL, Chen J, Neptune ER, Judge DP, Podowski M, Holm T, Meyers J, Leitch CC, Katsanis N, Sharifi N, et al. A syndrome of altered cardiovascular, craniofacial, neurocognitive and skeletal development caused by mutations in TGFBR1 or TGFBR2. Nat Genet 2005;37:275–281. [PubMed: 15731757]

Mehrara BJ, Spector JA, Greenwald JA, Ueno H, Longaker MT. Adenovirus-mediated transmission of a dominant negative transforming growth factor-[beta] receptor inhibits in vitro mouse cranial suture fusion. Plast Reconstr Surg 2002;110:506–514. [PubMed: 12142669]

Mommaerts MY, Staels PF, Casselman JW. The faith of a coronal suture grafted onto midline synostosis inducing dura and deprived from tensile stress. Cleft Palate Craniofac J 2001;38:533–537. [PubMed: 11522177]

Mooney MP, Burrows AM, Smith TD, Losken HW, Opperman LA, Dechant J, Kreithen AM, Kapucu R, Cooper GM, Ogle RC, et al. Correction of coronal suture synostosis using suture and dura mater allografts in rabbits with familial craniosynostosis. Cleft Palate Craniofac J 2001;38:206–225. [PubMed: 11386428]

Mooney MP, Burrows AM, Wigginton W, Singhal VK, Losken HW, Smith TD, Dechant J, Towbin A, Cooper GM, Towbin R. Intracranial volume in craniosynostotic rabbits. J Craniofac Surg 1998a; 9:234–239. [PubMed: 9693554]

Mooney MP, Fellows-Mayle W, Dechant J, Burrows AM, Smith TD, Cooper GM, Pollack I, Siegel MI. Increases in intracranial pressure following coronal suturectomy in rabbits with craniosynostosis. J Craniofac Surg 1999;10:104–111. [PubMed: 10388409]

Mooney MP, Losken HW, Moursi AM, Bradley J, Azari K, Acarturk TO, Cooper GM, Thompson B, Opperman LA, Siegel MI. Anti-TGF-beta2 antibody therapy inhibits postoperative resynostosis in craniosynostotic rabbits. J Plast Reconstr Surg 2007a;119:1200–1212.

Mooney MP, Losken HW, Moursi AM, Shand JM, Cooper GM, Curry C, Ho L, Burrows AM, Stelnicki EJ, Losee JE, et al. Postoperative anti-Tgf-beta2 antibody therapy improves intracranial volume and craniofacial growth in craniosynostotic rabbits. J Craniofac Surg 2007b;18:336–346. [PubMed: 17414283]

Mooney MP, Losken HW, Siegel MI, Lalikos JF, Losken A, Burrows AM, Smith TD. Development of a strain of rabbits with congenital simple, nonsyndromic coronal suture synostosis. Part II. Somatic and craniofacial growth patterns. Cleft Palate Craniofac J 1994a;31:8–14. [PubMed: 8130248]

Mooney MP, Losken HW, Siegel MI, Lalikos JF, Losken A, Smith TD, Burrows AM. Development of a strain of rabbits with congenital simple nonsyndromic coronal suture synostosis. Part I. Breeding demographics, inheritance pattern, and craniofacial anomalies. Cleft Palate Craniofac J 1994b;31:1–7. [PubMed: 8130237]

Mooney MP, Moursi AM, Opperman LA, Siegel MI. Cytokine therapy for craniosynostosis. Expert Opin Biol Ther 2004;4:279–299. [PubMed: 15006724]

Mooney MP, Siegel MI, Burrows AM, Smith TD, Losken HW, Dechant J, Cooper G, Fellows-Mayle W, Kapucu MR, Kapucu LO. A rabbit model of human familial, nonsyndromic, unicoronal suture synostosis: part 2: intracranial contents, intracranial volume, and intracranial pressure. Childs Nerv Syst 1998b;14:247–255. [PubMed: 9694336]

Mooney, MP.; Siegel, MI.; Opperman, LA. Animal models of craniosynostosis: Experimental, congenital, and transgenic. In: Mooney, MP.; Siegel, MI., editors. Understanding Craniofacial Anomalies: The Etiopathogenesis of Craniosynostosis and Facial Clefting. New York: J Wiley & Sons; 2002. p. 251-272.

Mooney MP, Smith TD, Burrows AM, Langdon HL, Stone CE, Losken HW, Caruso K, Siegel MI. Coronal suture pathology and synostotic progression in rabbits with congenital craniosynostosis. Cleft Palate Craniofac J 1996;33:369–378. [PubMed: 8891367]

Mouradian WE. Controversies in the diagnosis and management of craniosynostosis: a panel discussion. Cleft Palate Craniofac J 1998;35:190–193. [PubMed: 9603550]

Moursi AM, Winnard PL, Fryer D, Mooney MP. Delivery of transforming growth factor-β2-perturbing antibody in a collagen vehicle inhibits cranial suture fusion in calvarial organ culture. Cleft Palate Craniofac J 2003;40:225–232. [PubMed: 12733949]

Opperman LA, Adab K, Gakunga PT. Transforming growth factor-β2 and TGF-β3 regulate fetal rat cranial suture morphogenesis by regulating rates of cell proliferation and apoptosis. Dev Dyn 2000;219:237–247. [PubMed: 11002343]

Opperman LA, Chhabra A, Cho RW, Ogle RC. Cranial suture obliteration is induced by removal of transforming growth factor (TGF)-beta 3 activity and prevented by removal of TGF-beta 2 activity from fetal rat calvaria in vitro. J Craniofac Genet Dev Biol 1999;19:164–173. [PubMed: 10589398]

Opperman LA, Nolen AA, Ogle RC. TGF-β1, TGF-β2, and TGF-β3 exhibit distinct patterns of expression during cranial suture formation and obliteration in vivo and in vitro. J Bone Miner Res 1997;12:301–310. [PubMed: 9076572]

Opperman, LA.; Ogle, RC. Molecular studies of craniosynostosis: factors affecting cranial suture morphogenesis and patency. In: Mooney, MP.; Siegel, MI., editors. Understanding Craniofacial Anomalies: The Etiopathogenesis of Craniosynostosis and Facial Clefting. 1st ed.. New York: J Wiley & Sons; 2002. p. 497-518.

Panchal J, Uttchin V. Management of craniosynostosis. Plast Reconstr Surg 2003;111:2032–2048. [PubMed: 12711969]

Poisson E, Sciote JJ, Koepsel R, Cooper GM, Opperman LA, Mooney MP. Transforming growth factor-beta isoform expression in the perisutural tissues of craniosynostotic rabbits. Cleft Palate Craniofac J 2004;41:392–402. [PubMed: 15222795]

Pollack IF, Losken HW, Biglan AW. Incidence of increased intracranial pressure after early surgical treatment of syndromic craniosynostosis. Pediatr Neurosurg 1996;24:202–209. [PubMed: 8873162]

Premaraj S, Mundy B, Morgan D, Winnard PL, Mooney MP, Moursi AM. Sustained delivery of bioactive cytokine using a dense collagen gel vehicle. Arch Oral Biol 2006;51:325–333. [PubMed: 16226216]

Premaraj S, Mundy B, Parker-Barnes J, Winnard PL, Moursi AM. Collagen gel delivery of Tgf-beta3 non-viral plasmid DNA in rat osteoblast and calvarial culture. Orthod Craniofac Res 2005;8:320–322. [PubMed: 16238613]

Renier, D. Intracranial pressure in craniosynostosis: pre- and postoperative recordings—correlation with functional results. In: Persing, JA.; Edgerton, MT.; Jane, JA., editors. Scientific Foundations and Surgical Treatment of Craniosynostosis. Baltimore: Williams & Wilkins; 1989. p. 263-269.

Richtsmeier, JT. Cranial vault dysmorphology and growth in craniosynostosis. In: Mooney, MP.; Siegel, MI., editors. Understanding Craniofacial Anomalies: The Etiopathogenesis of Craniosynostoses and Facial Clefting. New York: J Wiley & Sons; 2002. p. 321-342.

Richtsmeier JT, Lele S. A coordinate-free approach to the analysis of growth patterns: models and theoretical considerations. Biol Rev 1993;68:381–411. [PubMed: 8347767]

Roth DA, Gold LI, Han VK, McCarthy JG, Sung JJ, Wisoff JH, Longaker MT. Immunolocalization of transforming growth factor β1, β2, and β3 and insulin-like growth factor I in premature cranial suture fusion. Plast Reconstr Surg 1997a;99:300–309. discussion 310–316. [PubMed: 9030135]

Roth DA, Longaker MT, McCarthy JG, Rosen DM, McMullen HF, Levine JP, Sung J, Gold LI. Studies in cranial suture biology: part I. Increased immunoreativity for TGF-β isoforms (β1, β2, and β3) during rat cranial suture fusion. J Bone Miner Res 1997b;12:311–321. [PubMed: 9076573]

Thompson DNP, Malcolm GP, Jones BM, Harkness WJ, Hayward RD. Intracranial pressure in single suture craniosynostosis. Pediatr Neurosurg 1995;22:235–240. [PubMed: 7547454]

Virchow R. Über den Cretinismus, namentlich in Franken, und über pathologische Schädelformen. Ver Phys Med Gesellsch Wurzburg 1851;2:230–270.

Warren SM, Brunet LJ, Harland RM, Economides AN, Longaker MT. The BMP antagonist noggin regulates cranial suture fusion. Nature 2003;422:625–629. [PubMed: 12687003]

Warren SM, Longaker MT. The pathogenesis of craniosynostosis in the fetus. Yonsei Med J 2001;42:646–659. [PubMed: 11754148]

Williams FL, Richtsmeier JT. Comparison of mandibular landmarks from computed tomography and 3D digitizer data. Clin Anat 2003;16:494–500. [PubMed: 14566895]

Yano H, Tanaka K, Sueyoshi O, Takahashi K, Hirata R, Hirano A. Cranial vault distraction: its illusionary effect and limitation. Plast Reconstr Surg 2006;117:193–200. [PubMed: 16404266]

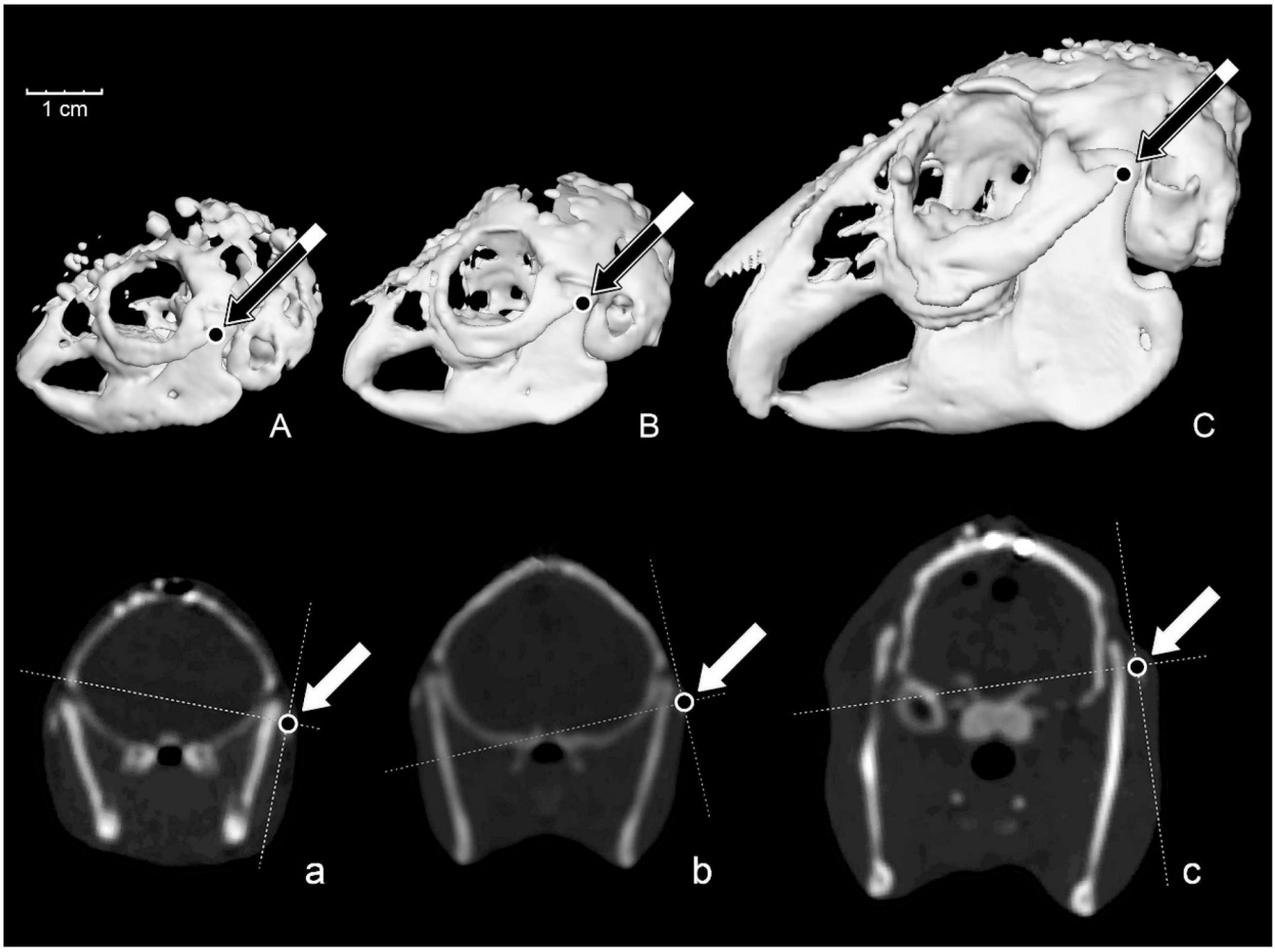

Figure 1.
Example three-dimensional (3D) reconstructions and CT slice data showing landmark identification. The example landmark on the posterior tip of the zygomatic bone is identified at each age, illustrating how landmarks are located using both 3D reconstructions and two-dimensional slice images in concert. Note the differences in overall size and extent of ossification at the three ages. A through C: Reconstructions of medical CT scans of rabbits used in this study at (A) 10 days, (B) 25 days, and (C) 84 days (scale bar: 1 cm). a through c: Coronal CT slice images corresponding to the reconstructions at (a) 10 days, (b) 25 days, and (c) 84 days (not to scale). Note: Each skull represents a single scan from our data sample and is not intended to reflect a mean form.

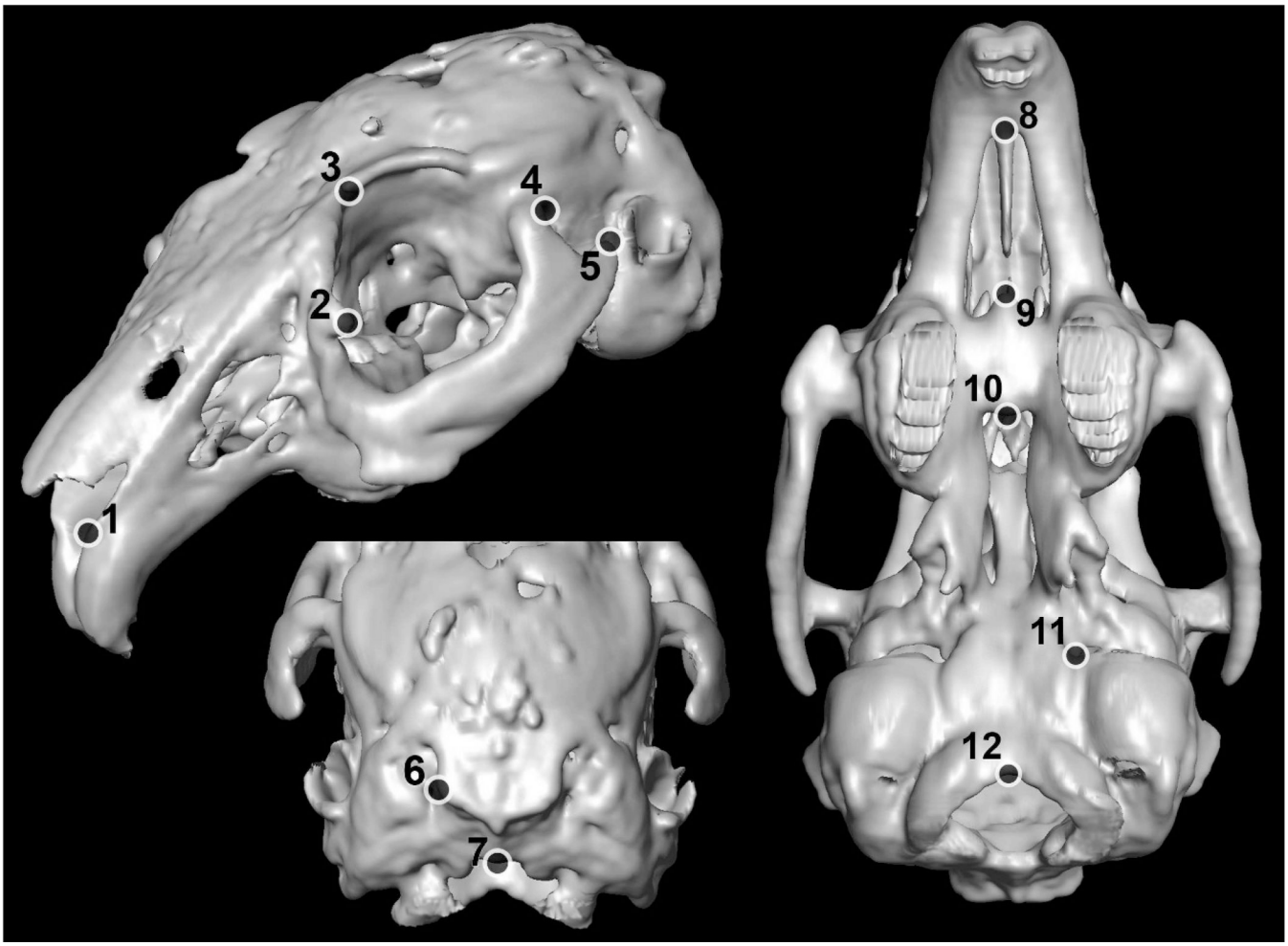

Figure 2.
Landmarks used in this study (see descriptions in Table 1), shown (from left) on lateral oblique, postero-dorsal, and ventral views of a CT reconstruction. For clarity, only midline and left-side landmarks are pictured here on an 84-day rabbit, although all landmarks were taken bilaterally (19 total) on all three age groups.

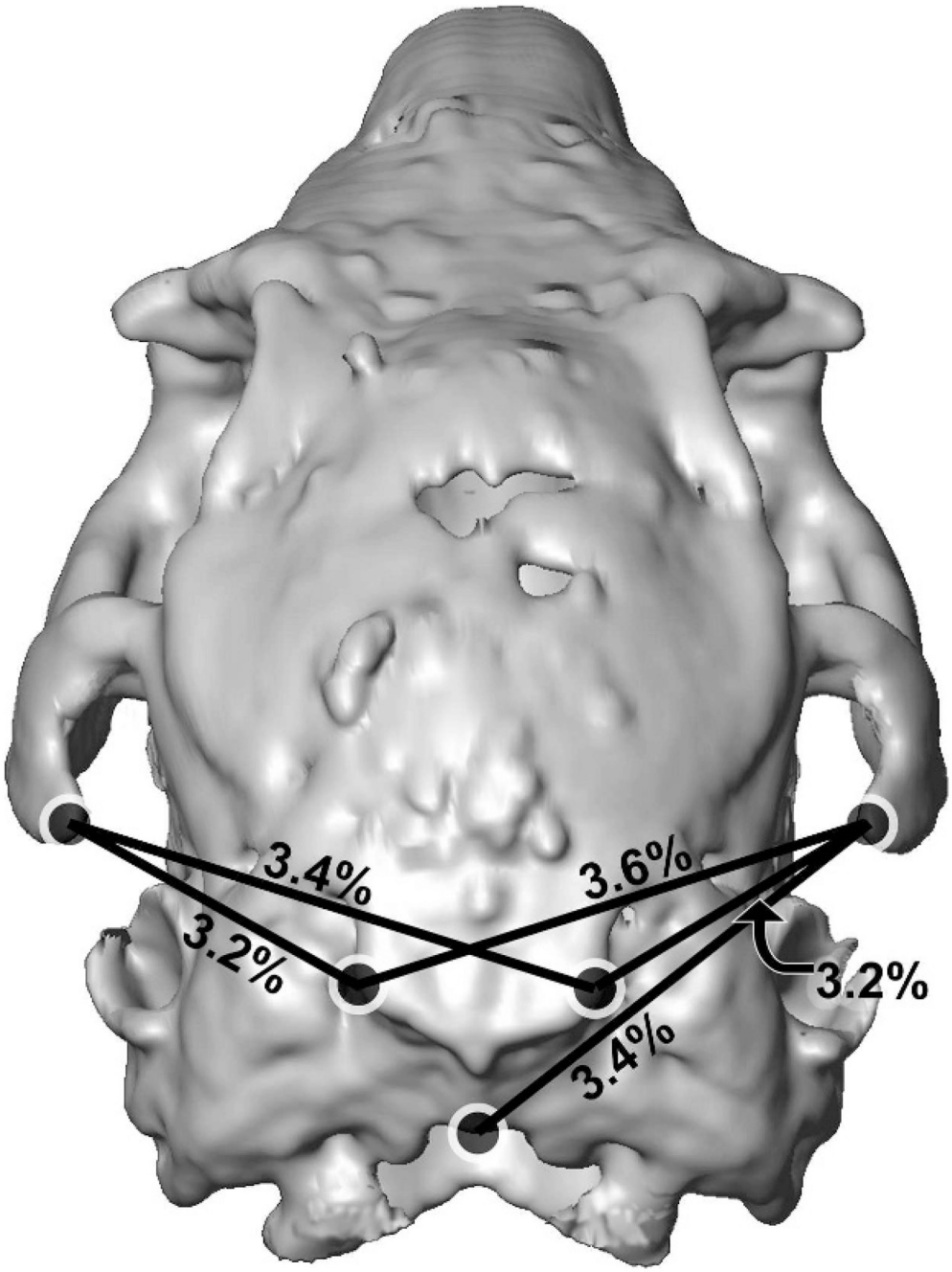

Figure 3.
Form differences between 25-day anti-Tgf-β2 and IgG control rabbits. Dorso-caudal view of skull. All lines represent distances in which anti–Tgf-β2 rabbits were larger than IgG control individuals. Magnitude of difference is indicated along each distance.

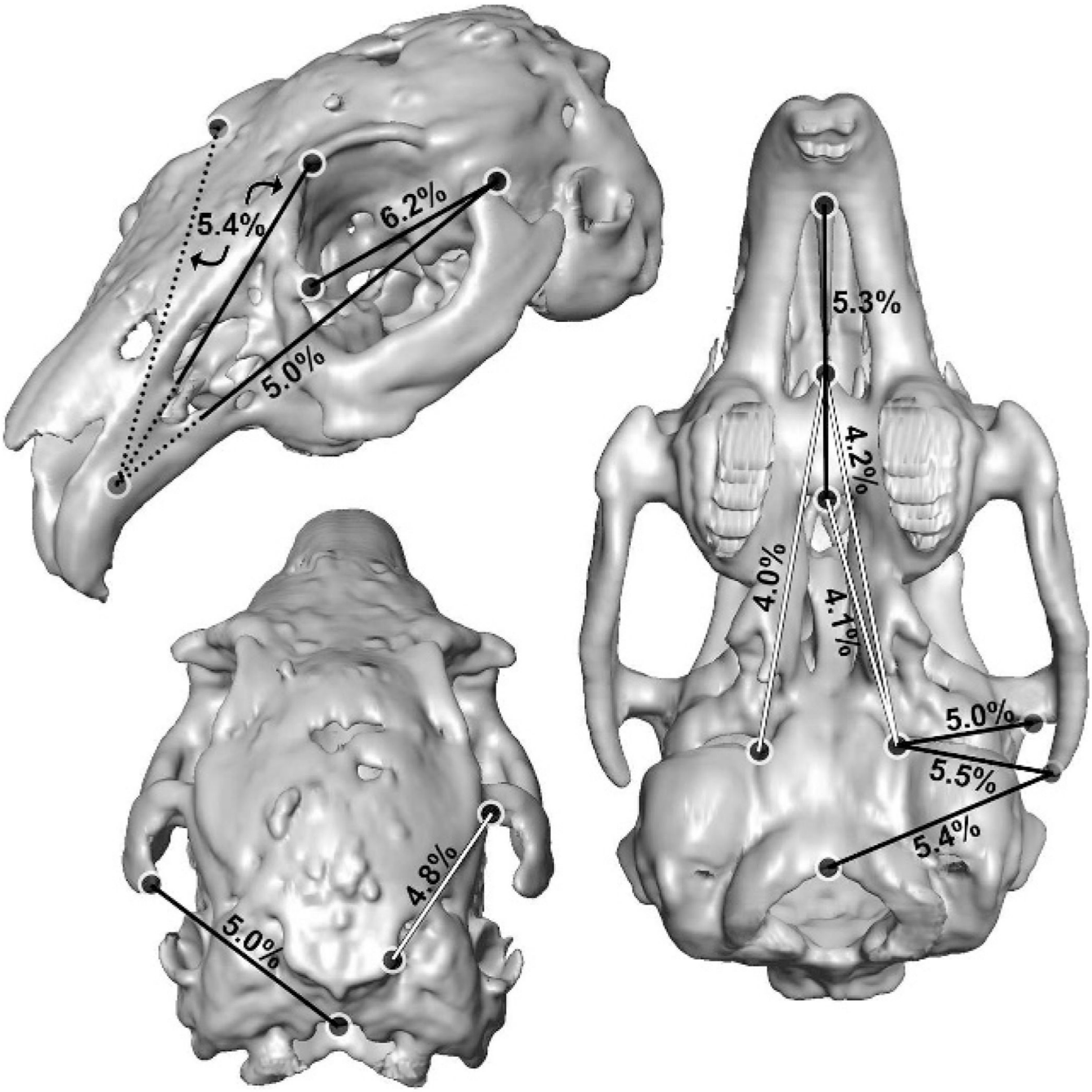

Figure 4.

Form differences between 84-day anti–Tgf-β2 rabbits and the two control groups. All lines represent distances that were greater in the anti–Tgf-β2 sample. Black lines indicate distances that were greater in the anti–Tgf-β2 sample than in suturectomy controls. White lines indicate distances that were greater in anti–Tgf-β2 rabbits than in IgG controls. Dotted lines indicate where the distance passes through bone. Magnitude of difference is indicated along each distance.

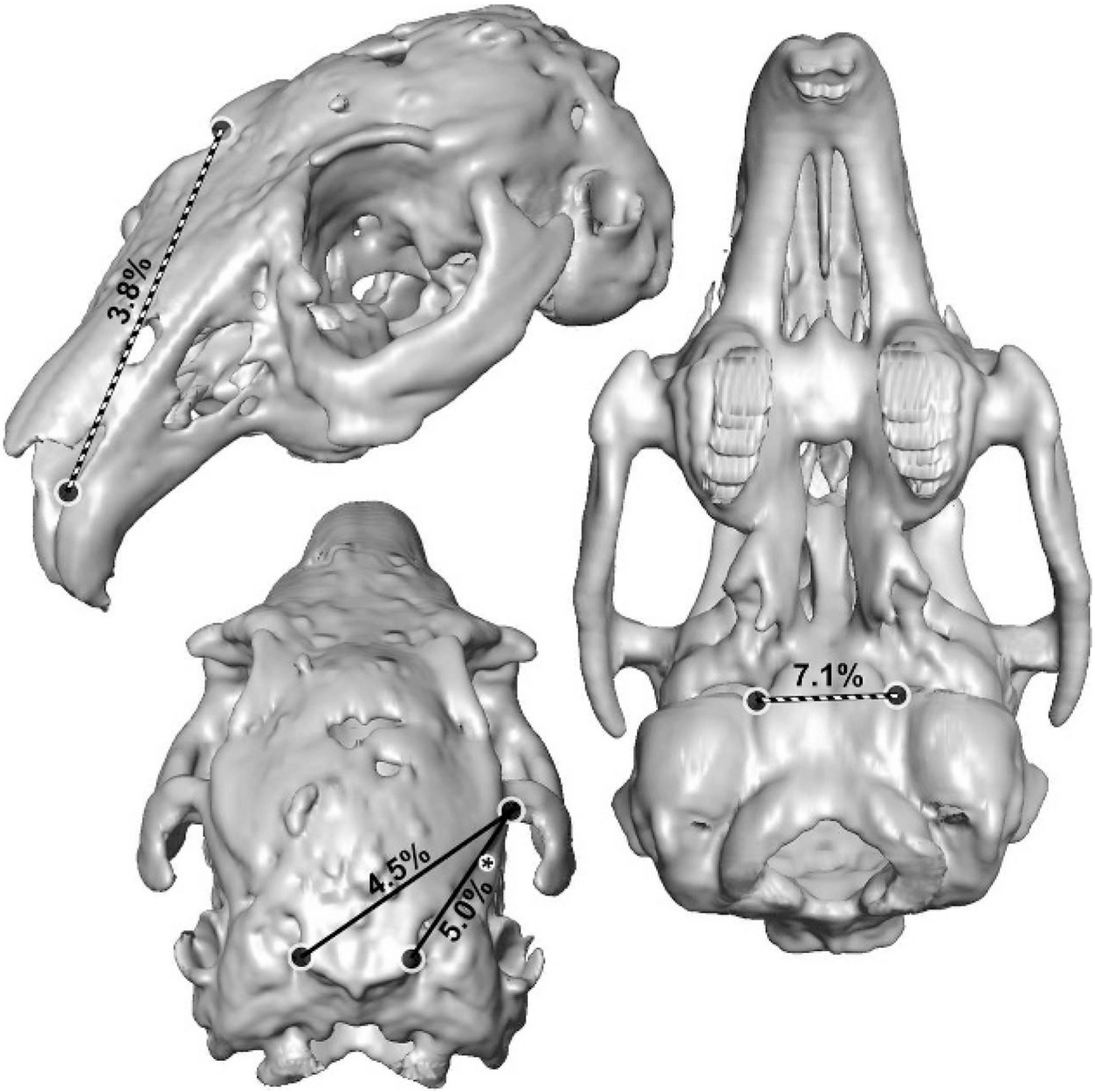

Figure 5.

Form differences between suturectomy control and IgG control rabbits at 84 days. Black lines represent distances that were larger in suturectomy control individuals, whereas striped lines represent distances that were larger in IgG controls. Magnitude of difference is indicated along each distance. The distance marked with an asterisk (*) indicates the lone distance in which a significant difference in growth is detected: (1) over the 25- to 84-day interval and 10- to 84-day interval in suturectomy control and IgG control rabbits, and (2) over the 10- to 84-day interval in anti–Tgf-β2 and IgG control rabbits.

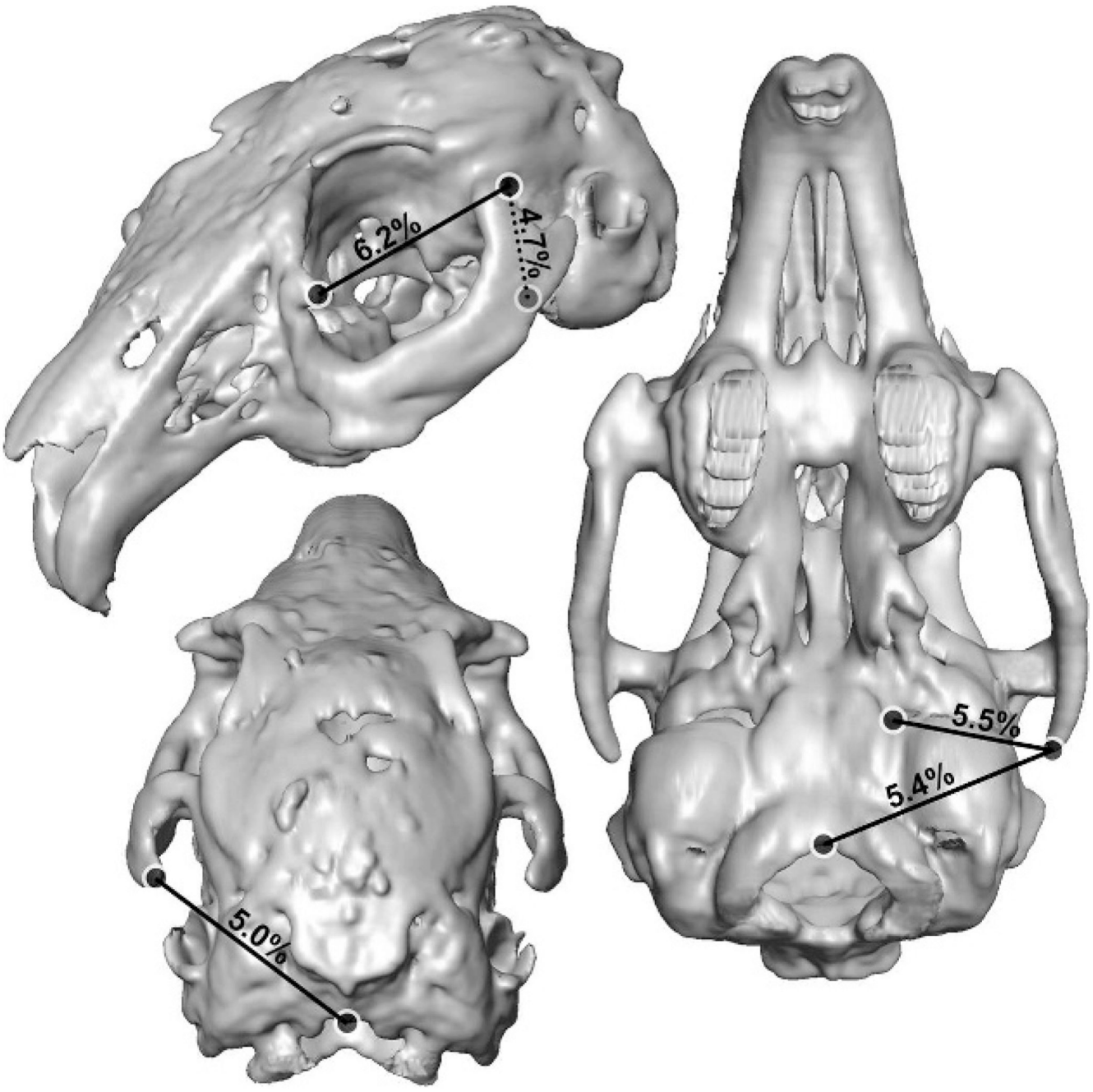

Figure 6.
Growth differences from 10 to 84 days. The anti–Tgf-β2 group grew significantly more than the suturectomy control group did in the illustrated distances. Dotted lines indicate where the distance passes through bone. Magnitude of difference is indicated along each distance.

TABLE 1

Craniofacial Landmarks Used in This Study*

1.	Left superior angle of incisive bone
2.	Left lacrimal process of lacrimal bone
3.	Left rostral supraorbital incisure
4.	Left neck of zygomatic process of temporal bone, posterior aspect
5.	Left posterior point of zygomatic bone
6.	Left lateral occipital protuberance
7.	Opisthion
8.	Anterior junction of palatine fissures
9.	Anterior point of intermaxillary suture
10.	Posterior point of interpalatal suture
11.	Left anterior junction of tympanic bulla and basal part of occipital
12.	Basion
13.	Right superior angle of incisive bone
14.	Right lacrimal process of lacrimal bone
15.	Right rostral supraorbital incisure
16.	Right neck of zygomatic process of temporal bone, posterior aspect
17.	Right posterior point of zygomatic bone
18.	Right lateral occipital protuberance
19.	Right anterior junction of tympanic bulla and basal part of occipital

* Numbers correspond to those in Figure 2. All landmarks were taken bilaterally, making 19 total. Only left-side and midline landmarks are pictured in Figure 2.

TABLE 2

Comparisons and Sample Sizes Described in This Study*

Intergroup Form Tests		**25 d**	**84 d**
		anti–Tgf-β2 (7) versus suturectomy control (6)	anti–Tgf-β2 (8) versus suturectomy control (7)
		anti–Tgf-β2 (7) versus IgG control (6)	anti–Tgf-β2 (8) versus IgG control (5)
		suturectomy control (6) versus IgG control (6)	suturectomy control (7) versus IgG control (5)
Intergroup Growth Tests	*10 to 25 d*†	*25 to 84 d*	*10 to 84 d*†
	anti–Tgf-β2 (7) versus suturectomy control (6)	anti–Tgf-β2 (7,8) versus suturectomy control (6,7)	anti–Tgf-β2 (8) versus suturectomy control (7)
	anti–Tgf-β2 (7) versus IgG control (6)	anti–Tgf-β2 (7,8) vs. IgG control (6,5)	anti–Tgf-β2 (8) versus IgG control (5)
	suturectomy (6) control versus IgG control (6)	suturectomy (6,7) control versus IgG control (6,5)	suturectomy control (7) versus IgG control (5)

*Sample sizes for each age and treatment group are noted in parentheses.

†The 10-day-old rabbits were pooled into a single group, n = 14. See “Materials and Methods” for further explanation.

TABLE 3

Sample Size for Each Age and Treatment Group, Based on Computed Tomography Scan Quality and Availability

	Anti-Tgf-β2	Suturectomy Control	IgG Control
Total individuals	11	8	6
10-day scans	5	7	2
25-day scans	7	6	6
84-day scans	8	7	5

TABLE 4

Significant Differences in Form Between Anti–Tgf-β2 and IgG Rabbits at 25 Days*

Distance	Location	Mean Distance: Anti–Tgf-β2 (mm)	Mean Distance: IgG (mm)	Mean Difference (%)
6 to 17	Posterior neurocranium	25.72	24.83	3.60
7 to 17	Posterior neurocranium	22.40	21.67	3.40
5 to 18	Posterior neurocranium	25.65	24.80	3.40
5 to 6†	Posterior neurocranium	20.87	20.21	3.20

*Each distance is indicated by its endpoints (landmark numbers correspond to those in Table 1). Distances are illustrated in Figure 3.

†This distance was also significantly different by 3.20% on the right side of the skull.

TABLE 5

Significant Differences in Form (of ≥4.0%) Between Anti–Tgf-B2 and Suturectomy Control Rabbits at 84 Days*

Distance	Location	Mean Distance: Anti–Tgf-β2 (mm)	Mean Distance: Suturectomy Control (mm)	Mean Difference (%)
2 to 4	upper face	23.01	21.65	6.2
5 to 11	lateral basicranium	16.40	15.55	5.5
3 to 8†	rostrum	41.96	39.86	5.4
5 to 12	lateral basicranium	25.09	23.82	5.4
10 to 8	palate	26.79	25.46	5.3
4 to 8	face	51.03	48.60	5.0
4 to 11	lateral basicranium	19.50	18.59	5.0
5 to 7	posterior cranium	24.83	23.67	5.0
14 to 11	midcranial height	38.32	36.55	4.8
14 to 10	face	21.91	20.91	4.8
2 to 11	midcranial height	32.96	31.46	4.7
5 to 6	posterior neurocranium	22.59	21.61	4.6
11 to 8†	basicranium	48.51	46.42	4.5
19 to 5	basicranium	26.46	25.37	4.4
14 to 3	upper face	27.37	26.21	4.4
16 to 8	face	51.19	49.07	4.4
11 to 9	basicranium	32.65	31.27	4.3
18 to 5	posterior neurocranium	29.54	28.39	4.2
13 to 4	face	55.72	53.48	4.2
13 to 11	cranial length	54.73	52.53	4.2
4 to 10	facial depth	27.81	26.70	4.2
4 to 9	facial depth	34.54	33.15	4.2
11 to 10	basicranium	22.97	22.05	4.1
3 to 10	facial depth	23.25	22.36	4.1
3 to 9	facial depth	25.75	24.76	4.1

*Each distance is indicated by its endpoints (landmark numbers correspond to those in Table 1). Distances in **bold** are illustrated by the black lines in Figure 4.

†These distances were also significantly different by a comparable amount on the right side.

TABLE 6

Significant Differences in Form (of ≥3.0%) Between Anti–Tgf-β2 and IgG Rabbits at 84 Days*

Distance	Location	Mean Distance: Anti–Tgf-β2 (mm)	Mean Distance: IgG (mm)	Mean Difference (%)
16 to 18	posterior neurocranium	24.33	23.22	4.8
11 to 9†	basicranium	32.65	31.28	4.2
11 to 10	basicranium	22.97	22.03	4.1
5 to 11	lateral basicranium	16.40	15.78	4.0
5 to 7	posterior cranium	24.83	23.87	4.0
12 to 9	basicranium	42.81	41.13	3.9
16 to 6	posterior neurocranium	30.15	29.00	3.9
4 to 11	lateral basicranium	19.50	18.78	3.9
11 to 8†	basicranium	48.51	46.70	3.8
2 to 11†	midcranial height	32.96	31.74	3.8
15 to 12	midcranial height	40.27	38.74	3.8
12 to 10	basicranium	32.93	31.69	3.7
12 to 8	basicranium	58.19	56.02	3.7
18 to 5	posterior neurocranium	29.54	28.54	3.6
19 to 10	basicranium	22.88	22.05	3.6
5 to 6	posterior neurocranium	22.60	21.85	3.4
5 to 12†	lateral basicranium	25.09	24.23	3.4
1 to 12†	cranial length	64.37	62.26	3.3
13 to 11	cranial length	54.73	52.95	3.3
14 to 12	midcranium	44.93	43.58	3.0

*Distances in bold are illustrated by the white lines in Figure 4.

†This distance was also significantly different on the right side of the skull (similar magnitude).

TABLE 7

Significant Differences in Form (of ≥3.0%) Between Suturectomy Control and IgG Control Rabbits at 84 Days*

Distance	Location	Mean Distance: Suturectomy Control (mm)	Mean Distance: IgG (mm)	Mean Difference (%)
16 to 18	posterior neurocranium	24.37	23.22	5.0
6 to 16	posterior neurocranium	30.32	29.00	4.5
1 to 15†	rostrum	42.68	44.24	3.8
11 to 19†	cranial base	11.06	11.80	7.1

*Distances are illustrated in Figure 5.

†Note that in these two distances, IgG control rabbits are larger than suturectomy controls at 84 days (striped lines in Fig. 5).

TABLE 8

Significant Differences in Growth Between Anti–Tgf-B2 and Suturectomy Control Rabbits From 10 to 84 Days*

		Mean Distance: Anti–Tgf-β2 (mm)		Mean Distance: Suturectomy Control (mm)		Mean Difference in Growth	
Distance	**Location**	**10 d**	**84 d**	**10 d**	**84 d**	**mm**	**%**
2 to 4	upper face	13.77	23.01	13.77	21.65	1.36	6.2
5 to 11	lateral basicranium	11.84	16.40	11.84	15.55	0.85	5.5
5 to 12	lateral basicranium	17.40	25.09	17.40	23.82	1.27	5.4
5 to 7	posterior cranium	20.50	24.83	20.50	23.67	1.16	5.0
2 to 11	midcranial height	19.82	32.96	19.82	31.46	1.50	4.7

*Distances are illustrated in Figure 6.